

# Gaplike behavior of the $c$ -axis dynamic conductivity in pure and Ti-doped $\text{Sr}_2\text{RuO}_4$

K. Pucher,<sup>1</sup> A. Loidl,<sup>1</sup> N. Kikugawa,<sup>2</sup> and Y. Maeno<sup>2,3</sup>

<sup>1</sup>*Experimentalphysik V, Elektronische Korrelationen und Magnetismus, Institut für Physik, Universität Augsburg, D-86135 Augsburg, Germany*

<sup>2</sup>*Department of Physics, Kyoto University, Kyoto 606-8502, Japan*

<sup>3</sup>*Kyoto University International Innovation Center, Kyoto 606-8501, Japan*

(Received 16 September 2003; published 9 December 2003)

We report on infrared spectroscopy of the interplane reflectivity of pure and Ti-doped  $\text{Sr}_2\text{RuO}_4$  single crystals. The electronic part of the dynamic conductivity can be well described by a two component model, which consists of a coherent part, using the standard Drude model, and a mid-infrared peak. The scattering rate in  $\text{Sr}_2\text{RuO}_4$  exhibits a gaplike behavior with a gap energy of 6.3 meV. On Ti doping we observe a reduction of the gap, which is fully closed for  $x=0.05$ . We discuss the origin of the gap and the suppression by Ti doping on the basis of magnetic origin as well as of a dimensional crossover in the charge transport.

DOI: 10.1103/PhysRevB.68.214502

PACS number(s): 74.70.Pq, 71.27.+a, 72.30.+q, 78.30.-j

## I. INTRODUCTION

The layered perovskite  $\text{Sr}_2\text{RuO}_4$  has attracted considerable attention since the discovery of superconductivity at  $T_c \approx 1.4$  K.<sup>1</sup> Early theoretical suggestions about  $p$ -wave superconductivity<sup>2,3</sup> have been corroborated by a number of experimental observations.<sup>4-6</sup> But despite some similarities with superfluid  $^3\text{He}$  and the search for ferromagnetic (FM) spin fluctuations, the pairing mechanism could not be established.<sup>7</sup> NMR measurements in the normal conducting state established the existence of antiferromagnetic (AFM) spin fluctuations, which are strongly anisotropic and related to the Fermi-surface nesting of the quasi-one-dimensional  $d_{xz}$  bands and  $d_{yz}$  bands.<sup>8</sup> These observations are consistent with quasi-elastic neutron-scattering results demonstrating the existence of incommensurate spin fluctuations.<sup>9</sup>

In addition to the superconducting properties, also the normal-conducting state received equal attention. At low temperatures  $\text{Sr}_2\text{RuO}_4$  reveals a metallic behavior along all directions, but the in- and interplane resistivities ( $\rho_{ab}$  and  $\rho_c$ ) are anisotropic with  $\rho_c/\rho_{ab} \approx 2000$ . Both, the in- and interplane resistivities follow  $\rho = AT^2$ , however with  $A_c/A_{ab} \approx 10^3$  yielding a strongly anisotropic three-dimensional (3D) or quasi-2D Fermi liquid (FL).<sup>10</sup> The interplane resistivity exhibits a crossover to a semiconducting  $T$  dependence at  $T^* \approx 100$  K, while  $\rho_{ab}$  continuously increases up to  $T = 1300$  K, far beyond the Ioffe-Regel limit.<sup>11</sup>

A “bad metallic” in-plane transport,<sup>12</sup> together with a nonmetallic  $T$  dependence of the interplane transport was observed in many layered transition metal oxides, e.g., high- $T_c$  cuprates. In addition, the description of the dynamic conductivity  $\sigma(\omega)$  in these systems failed using a standard Drude model (SDM), due to additional spectral weight in the mid-infrared (MIR) range. These anomalous transport properties can be reproduced either by assuming a strongly anisotropic in- and interplane scattering rate<sup>13</sup> (indeed detailed studies of the Fermi surface of  $\text{Sr}_2\text{RuO}_4$  reveal a strongly  $k$ -dependent interplane transport, which is dominated by the  $\beta$  sheet, while the in-plane transport mainly arises from the  $\gamma$  sheet<sup>14</sup>), or by dynamic mean-field theory,<sup>15</sup> where the

charge dynamics consist mainly of two components: (i) a sharp Drude peak (formed by coherent quasi particle excitation) and (ii) a broad, almost  $T$ -independent contribution (from incoherent excitations) at higher frequencies.

First optical studies on  $\text{Sr}_2\text{RuO}_4$  reflected the strong anisotropic charge dynamic in the system.<sup>16</sup> Later on the far-infrared (FIR)  $c$ -axis reflectance on “3-K phase” samples, where inclusion of lamellar microdomains of ruthenium metal leads to an enhancement of  $T_c$  up to 3 K,<sup>17</sup> were investigated by Hildebrand *et al.*<sup>18</sup> using an extended Drude model (EDM), which assumes frequency dependencies of effective mass  $m^*$  and scattering rate  $\gamma$ . They observed a suppression of the scattering rate around 8 meV at low temperatures. Preliminary results on the  $c$ -axis charge dynamics of highly pure  $\text{Sr}_2\text{RuO}_4$  single crystals were also given in Ref. 19.

In order to clarify the origin of the scattering mechanism in  $\text{Sr}_2\text{RuO}_4$  we performed a series of infrared (IR) reflectivity measurements on  $\text{Sr}_2\text{Ru}_{1-x}\text{Ti}_x\text{O}_4$  with  $0 \leq x \leq 0.05$ . The substitution of  $\text{Ru}^{4+}$  with nonmagnetic  $\text{Ti}^{4+}$  results in a strong enhancement of  $\rho_{ab}$ , which increases towards low temperatures for higher  $x$ .<sup>20,21</sup> The  $c$ -axis transport reveals a purely semiconducting behavior for  $x > 0.05$  below room temperature. Already at low doping levels the magnetic susceptibility  $\chi_m$  exhibits a Curie-Weiss behavior, with a strong Ising-like anisotropy and undergoes a spin-glass transition at  $T_m \approx 10$  K.<sup>20,21</sup> In neutron-scattering experiments incommensurate fluctuations were detected evolving into a spin-density wave (SDW) at low temperatures.<sup>22</sup>

## II. EXPERIMENTAL DETAILS

Single crystals of  $\text{Sr}_2\text{Ru}_{1-x}\text{Ti}_x\text{O}_4$  with  $x = 0, 0.001, \text{ and } 0.05$  were grown by the floating-zone melting technique in a IR image furnace.<sup>23,20</sup> The pure  $\text{Sr}_2\text{RuO}_4$  sample reveals superconductivity below  $T_c = 1.43$  K, the 0.1% sample below 0.62 K, while superconductivity is totally suppressed for  $x \geq 0.0015$ .<sup>24</sup> There is no indication of the inclusion of the 3-K phase in the samples used in this study. The samples examined in this work were rods with typical dimensions of 3–7 mm in  $ab$  direction and 2–3 mm in  $c$  direction. The

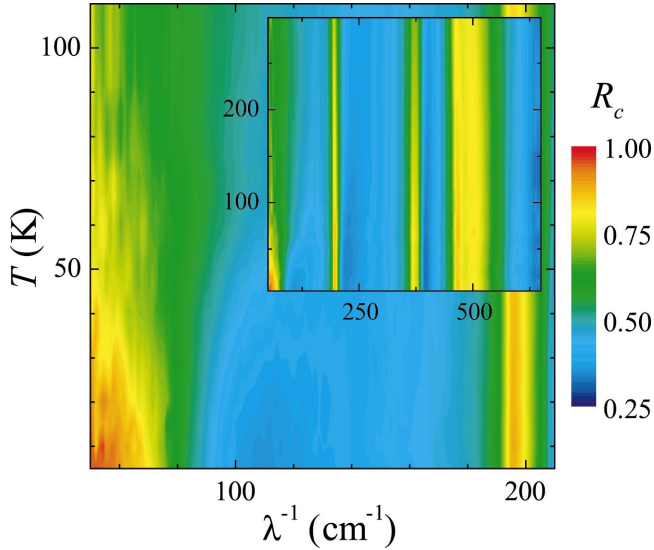


FIG. 1. (Color) Contour plot of the low-energy  $c$ -axis reflectivity  $R_c$  of pure  $\text{Sr}_2\text{RuO}_4$  ( $T_c=1.43$  K) vs temperature and wave number (derived from interpolation of 15 measured spectra). The inset shows  $R_c$  within the whole FIR range.

measurements of the optical reflectivity were carried out on polished single crystals using a Fourier-transformation IR spectrometer with a full bandwidth of 10–8000  $\text{cm}^{-1}$  (Bruker IFS 113v) together with a  $^4\text{He}$  cryostat (Oxford Optistat) in the range of 5 K  $< T < 300$  K. For the orientation of the samples we use a IR microscope (Bruker IRscope II).

### III. RESULTS AND DISCUSSION

Figure 1 shows the interplane reflectivity  $R_c$  as obtained for pure  $\text{Sr}_2\text{RuO}_4$  in a 2D-contour plot vs wave numbers  $\lambda^{-1}$  and  $T$ . The inset gives an overview of the full FIR range and the phonons can easily be observed as bright vertical lines, associated with the three  $A_u$  modes at 196, 358, and 465  $\text{cm}^{-1}$ .<sup>25</sup> All phonon modes are only weakly  $T$  dependent. Between 150 K  $< T < 300$  K the reflectivity increases below 150  $\text{cm}^{-1}$ , which is characteristic for lightly doped semiconductors or bad metals. But at the low temperatures  $R_c$  increases towards 1 and becomes minimal close to 100  $\text{cm}^{-1}$  indicating a well defined plasma edge. The results immediately signal a very small interplane Drude weight, but also a very low  $\gamma$ , prerequisites for the clear experimental signature of a plasma edge.

For a quantitative analysis we directly fitted  $R_c$ . We were unable to describe  $R_c$  utilizing a SDM plus Lorentzian for the phonons, due to missing spectral weight in the MIR. As mentioned before, earlier analysis on  $\text{Sr}_2\text{RuO}_4$  used a EDM to solve this problem.<sup>16,18</sup> Here we use a two-component model, consisting of a  $T$ -dependent coherent (SDM) and a  $T$ -independent incoherent (broad Lorentzian) contribution (details given in Ref. 26). Our investigations reveal that the incoherent part remains unchanged for  $T < 100$  K. Although we cannot exclude a small shift from the coherent to incoherent contribution for  $T > 100$  K, we feel that a two-component analysis is straightforward and provides excellent fits.

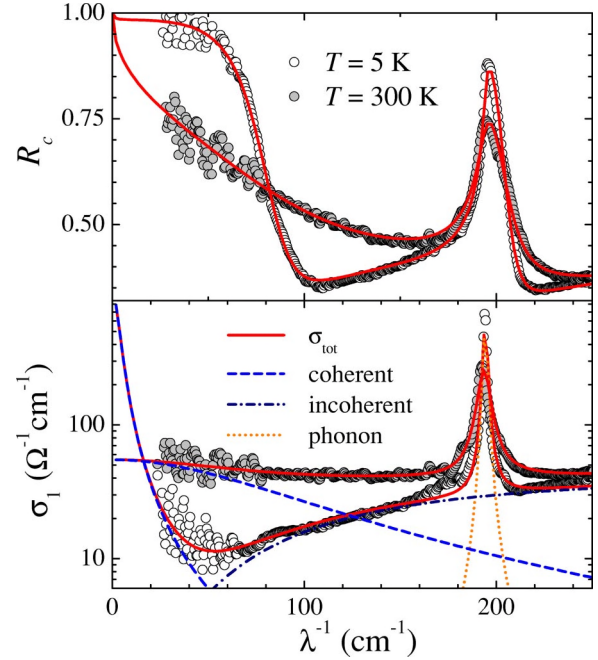


FIG. 2. (Color online) Low frequency  $c$ -axis reflectivity (upper frame) and conductivity (lower frame, semilogarithmic representation) vs wave number  $\text{Sr}_2\text{RuO}_4$  at room temperature and 5 K. The solid lines are the results of fits as described in the text. In the lower frame the different contributions (coherent Drude-like contributions—dashed lines, incoherent contribution—dash-dotted line, and phonon contribution—dotted line) are indicated separately.

The upper frame of Fig. 2 shows the remarkable agreement between these fits (solid lines) and the measured  $R_c$  at 5 and 300 K for  $\lambda^{-1} \leq 250$   $\text{cm}^{-1}$ . In the lower frame the conductivity is shown as function of wave number in a semi-logarithmic representation. In this case the optical conductivity was calculated from a Kramers-Kronig analysis of  $R_c$  assuming a Hagen-Rubens extrapolation towards zero wave number. Again the results of the fits are shown as solid lines. The different contributions for  $T=5$  and 300 K, namely the SDM (dashed lines), the incoherent (dash-dotted line), and the phonon (dotted line) contribution are shown separately. The lower frame of Fig. 2 provides clear experimental evidence that an incoherent part, not included in the previous reports, is absolutely necessary to describe the dynamic conductivity in  $\text{Sr}_2\text{RuO}_4$  agreeing well with theoretical predictions (e.g., Ref. 15) and confirming the two-component model.

As mentioned above, the incoherent contribution was assumed  $T$  independent using a resonance frequency of 2000  $\text{cm}^{-1} \approx 248$  meV, a damping of 26 500  $\text{cm}^{-1} \approx 3.3$  eV, and an optical dielectric permittivity  $\epsilon_\infty = 5.5$ . The Drude conductivity  $\sigma_1(\omega) = \sigma_{dc} / (1 + \omega^2 \tau^2)$  was fitted with a  $T$ -dependent dc conductivity  $\sigma_{dc} = e^2 N \tau / m^*$  and a  $T$ -dependent, but  $\omega$ -independent scattering rate  $\gamma = 1/\tau$ . From these fits the  $T$  dependence of  $\gamma$ ,  $\sigma_{dc}$ , and  $\omega_p = [e^2 N / (\epsilon_0 m^*)]^{1/2}$  can be unambiguously derived and the results are shown in Fig. 3. The plasma frequency (upper frame, left scale) is only weakly  $T$  dependent and decreases from 570  $\text{cm}^{-1} \approx 71$  meV at room temperature to

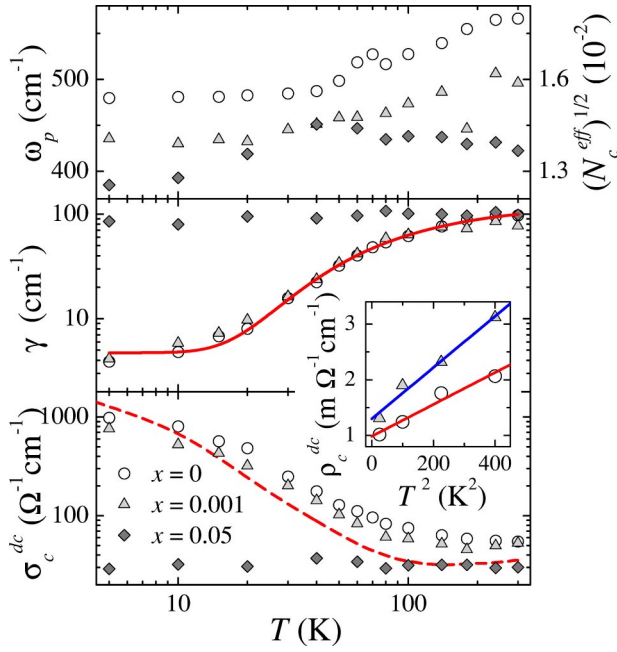


FIG. 3. (Color online) Temperature dependence of the fit parameter  $\omega_p$ ,  $\gamma$ , and  $\sigma_c^{dc}$  as obtained from the standard Drude model for  $\text{Sr}_2\text{Ru}_{1-x}\text{Ti}_x\text{O}_4$ . The solid line in the middle panel is given by fitting the data using Eq. (1). The interplane dc conductivity for  $x=0$  measured by four-probe technique<sup>20</sup> is indicated as dashed line in the lower panel. The inset shows  $\rho_c = 1/\sigma_c^{dc}$  vs  $T^2$  at low temperatures including fit results (solid lines).

$480 \text{ cm}^{-1} \approx 60 \text{ meV}$  at 5 K. The interplane dc conductivity (Fig. 3, lower frame) is almost constant above 100 K, and strongly increases below 100 K. It closely follows  $\sigma_c^{dc}$  as measured via four-probe techniques (dashed line). The effective number of charge carriers participating in the coherent transport along  $c$ ,  $N_c^{eff}$ , (upper frame, right scale) can directly be derived from  $\omega_p$  and is of the order of  $3 \times 10^{-4}$ , 15 times lower compared to the value determined by band-structure calculations.<sup>27</sup> However, at low temperatures the anisotropy  $N_{ab}^{eff}/N_c^{eff} \approx 2 \times 10^3$  (where  $N_{ab}^{eff}$  is taken from Ref. 16) is in agreement with the obtained dc ratio.<sup>24</sup> We estimate the mean free path of the charge carriers  $l_c = v_F/\gamma$  using the Fermi velocity  $v_F$  from Ref. 27. We find  $l_c = 1198 \text{ \AA}$  (48  $\text{\AA}$ ) at  $T=5 \text{ K}$  (300 K), enhanced by one order of magnitude when compared to the results from Mackenzie *et al.*<sup>28</sup> This enhancement can be partly attributed to the improvement of the crystal quality. But it is also well known that band-structure calculations often overestimate the interplane Fermi velocity giving too large mean-free-path values  $l_c$ .

However, the most fascinating  $T$  dependence is observed in the scattering rate  $\gamma$ , which can be described by an exponential decrease towards low temperatures (middle frame of Fig. 3):

$$\gamma(T) = \gamma_0 + \gamma_1 e^{-\Delta/T}. \quad (1)$$

Here a thermally activated behavior with a gap energy of  $\Delta = 74 \text{ K} \approx 51 \text{ cm}^{-1} \approx 6.3 \text{ meV}$ ,  $\gamma_0 = 4.7 \text{ cm}^{-1}$  and  $\gamma_1 = 121 \text{ cm}^{-1}$  reproduces almost perfectly the observations

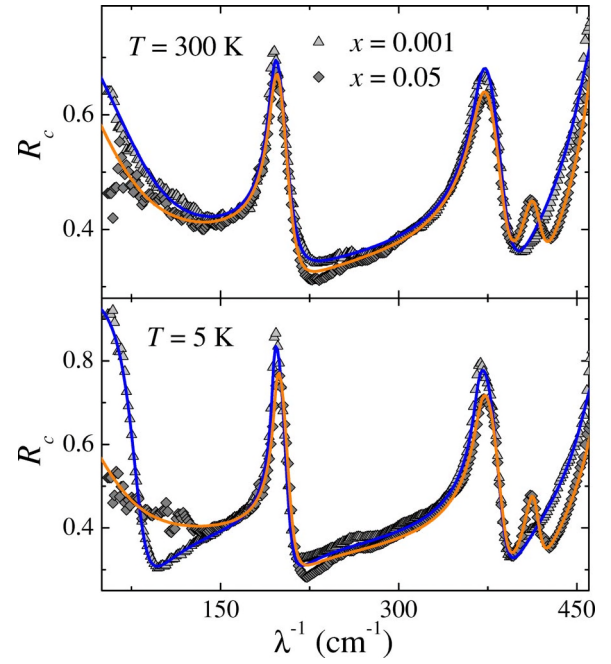


FIG. 4. (Color online) FIR  $c$ -axis reflectivity of  $\text{Sr}_2\text{Ru}_{1-x}\text{Ti}_x\text{O}_4$  with  $x=0.001$  and  $0.05$  at  $T=300 \text{ K}$  (upper panel) and  $5 \text{ K}$  (lower panel). The solid lines are results of the fits.

in the complete temperature range investigated. Figures 1–3 suggest a gaplike behavior of the relaxation rate that dominates  $\rho_c$  at least up to room temperature and the incoherent transport plays a minor role. But certainly at low temperatures,  $\rho_c$  can also be described using the FL ansatz  $\rho_c = \rho_0 + A_c T^2$  (solid lines in inset of Fig. 3) with an interplane conductivity coefficient  $A_c = 2.9 \mu\Omega \text{ cm/K}^2$  ( $4.6 \mu\Omega \text{ cm/K}^2$ ) for  $x=0$  ( $0.001$ ), both values in agreement with dc measurements.<sup>10</sup>

Finally Fig. 4 shows  $R_c$  as measured at  $T=300 \text{ K}$  (upper frame) and  $5 \text{ K}$  (lower frame) for two Ti-doped samples with  $x=0.001$  (bold triangles) and  $x=0.05$  (full rhombus). At first sight the spectra for  $x=0$  ( $T_c=1.43 \text{ K}$ ) and  $x=0.001$  ( $T_c=0.62 \text{ K}$ ) look rather similar. A closer inspection at  $5 \text{ K}$  reveals that  $\omega_p$  is slightly reduced for  $x=0.001$ , indicating that  $N_c^{eff}$  becomes reduced. For  $x=0.05$  the  $T$  dependence of  $R_c$  is rather weak and the evolution of a plasma edge is fully suppressed. The scattering rate remains large for all temperatures.

The strength of all phonon becomes slightly reduced on increasing  $x$  and a new phonon close to  $410 \text{ cm}^{-1}$  becomes apparent. The strength of this impurity mode increases with Ti doping and can probably be assigned to the Ti-O bending mode. The  $T$  dependencies of  $R_c$  for  $x=0.001$  and  $0.05$  have been fitted as outlined above and the resulting parameters have been included in Fig. 3. The plasma frequency and concomitantly  $N_c^{eff}$  are significantly reduced on Ti doping, which either is caused by a shift of coherent towards incoherent transport or by an enhancement of the effective mass  $m^*$ . For  $x=0.001$  the scattering rate closely follows the results observed for  $x=0$ , but always being slightly enhanced, resulting in a decrease of  $\sigma_c^{dc}$  in good agreement with four-probe dc results.<sup>20</sup> Using Eq. (1) the  $T$  dependence of  $\gamma$  for

$x=0.001$  was fitted, yielding a slightly reduced gap of  $\Delta = 4.8$  meV. For  $x=0.05$  the scattering rate remains large and almost  $T$  independent, indicating that the gap now has been finally closed. As a matter of fact, at low temperatures, the  $c$ -axis conductivity becomes significantly reduced on Ti doping. For  $x=0.05$  the dc values are only weakly  $T$  dependent and at 5 K reduced by almost a factor 50 when compared to  $x=0$ , again in reasonable agreement with the dc measurements.<sup>20</sup>

#### IV. CONCLUSION

In conclusion our data provide clear experimental evidence that an interpretation of the dynamic interplane conductivity in terms of two components is adequate. In particular the separation into a narrow strongly  $T$ -dependent coherent and a broad  $T$ -independent incoherent contribution is straightforward. We want to outline two possible scenarios to explain the coherent transport properties.

The strong increase of coherent  $c$ -axis conductivity below 100 K results from an abrupt and strong decrease of  $\gamma$ . What is the microscopic origin of this unusual  $T$  dependence? It could be the coupling to gapped magnetic excitations, reminiscent to the pseudogap behavior in the high- $T_c$  cuprates. However, neither by NMR nor by neutron scattering a gap-like behavior of spin fluctuations has been observed. The spectrum is dominated by ungapped AFM spin fluctuations arising from Fermi-surface nesting. A correlation between the freezing of spin fluctuations and the suppression of  $\gamma$  can be excluded on the basis of our experiments. A spin-density wave evolves on Ti doping, e.g.,  $T_m \approx 6$  K for  $x=0.05$ , but in this case the scattering rate is  $T$  independent as documented in Fig. 3. Of course, the anomalous electronic scattering rate could result from the coupling to so far unob-

served FM fluctuations peaked about  $q=0$ , which of course is a mere speculation. Very recently, a gaplike structure in the density of states with a width of 5 meV has been observed by tunneling microscopy in pure and lightly ( $x=0.00125$ ) doped  $\text{Sr}_2\text{Ru}_{1-x}\text{Ti}_x\text{O}_4$ .<sup>29</sup> The size of the gap seems to be in the order of our observation, however, the nature of the gap remains unexplained.

A more intriguing explanation could be that at low temperatures  $\text{Sr}_2\text{RuO}_4$  behaves like a strongly anisotropic but essentially 3D Fermi liquid, where the 2D Ru-O planes are coupled via the coherent  $c$ -axis transport to a 3D whole. This change in the effective dimensionality correlates with the presence of coherent quasiparticles in all three dimensions as has been observed recently by Valla *et al.* in layered cobaltates.<sup>30</sup> On increasing temperature the scattering rate increases Fermi-liquid-like proportional to  $T^2$ , but when the mean free path decreases to the order of the interplane separation, in-plane scattering processes start to dominate the  $c$ -axis transport. That implies several in-plane scattering events of the charge carriers between two successive interplane tunneling transitions and therefore the loss of phase coherence which explain the almost  $T$ -independent scattering rate along  $c$  at higher temperatures.

#### ACKNOWLEDGMENTS

The authors thank S. Kehrein, T. Pruschke, M. Braden, D.J. Singh, and M. Sigrist for helpful discussions and F. Mayr for the experimental support. This work was partly supported by the DFG via the Sonderforschungsbereich 484 (Augsburg), by the BMBF via the Contract No. EKM/13N6917/0, and by Grants-in-Aid from the Japan Society for Promotion of Science and from the Ministry of Education, Culture, Sports, Science, and Technology of Japan.

<sup>1</sup>Y. Maeno, H. Hashimoto, K. Yoshida, S. NishiZaki, T. Fujita, J.G. Bednorz, and F. Lichtenberg, *Nature (London)* **372**, 532 (1994).

<sup>2</sup>T.M. Rice and M. Sigrist, *J. Phys.: Condens. Matter* **7**, L643 (1995).

<sup>3</sup>G. Baskaran, *Physica B* **223-224**, 490 (1996).

<sup>4</sup>K. Ishida, H. Mukuda, Y. Kitaoka, K. Asayama, Z.Q. Mao, Y. Mori, and Y. Maeno, *Nature (London)* **396**, 658 (1998).

<sup>5</sup>G.M. Luke, Y. Fudamoto, K.M. Kojlma, M.I. Larkin, J. Merrin, B. Nachumi, Y.J. Uemura, Y. Maeno, Z.Q. Mao, Y. Mori, H. Nakamura, and M. Sigrist, *Nature (London)* **394**, 558 (1998).

<sup>6</sup>A.P. Mackenzie, R.K.W. Haselwimmer, A.W. Tyler, G.G. Lonzarich, Y. Mori, S. NishiZaki, and Y. Maeno, *Phys. Rev. Lett.* **80**, 161 (1998).

<sup>7</sup>Y. Maeno, T.M. Rice, and M. Sigrist, *Phys. Today* **54**, 42 (2001); A.P. Mackenzie and Y. Maeno, *Rev. Mod. Phys.* **75**, 657 (2003).

<sup>8</sup>K. Ishida, H. Mukuda, Y. Minami, Y. Kitaoka, Z.Q. Mao, H. Fukazawa, and Y. Maeno, *Phys. Rev. B* **64**, 100501 (2001), and references therein.

<sup>9</sup>Y. Sidis, M. Braden, P. Bourges, B. Hennion, S. NishiZaki, Y. Maeno, and Y. Mori, *Phys. Rev. Lett.* **83**, 3320 (1999).

<sup>10</sup>Y. Maeno, K. Yoshida, H. Hashimoto, S. NishiZaki, S. Ikeda, M.

Nohara, T. Fujita, A.P. Mackenzie, N.E. Hussey, J.G. Bednorz, and F. Lichtenberg, *J. Phys. Soc. Jpn.* **66**, 1405 (1997).

<sup>11</sup>A.W. Tyler, A.P. Mackenzie, S. NishiZaki, and Y. Maeno, *Phys. Rev. B* **58**, R10 107 (1998).

<sup>12</sup>V.J. Emery and S.A. Kivelson, *Phys. Rev. Lett.* **74**, 3253 (1995).

<sup>13</sup>L.B. Ioffe and A.J. Millis, *Phys. Rev. B* **58**, 11 631 (1998); D. van der Marel, *ibid.* **60**, R765 (1999).

<sup>14</sup>C. Bergemann, S.R. Julian, A.P. Mackenzie, S. NishiZaki, and Y. Maeno, *Phys. Rev. Lett.* **84**, 2662 (2000).

<sup>15</sup>T. Pruschke, D.L. Cox, and M. Jarrell, *Phys. Rev. B* **47**, 3553 (1993); J. Merino and R.H. McKenzie, *ibid.* **61**, 7996 (2000).

<sup>16</sup>T. Katsufuji, M. Kasai, and Y. Tokura, *Phys. Rev. Lett.* **76**, 126 (1996).

<sup>17</sup>Y. Maeno, T. Ando, Y. Mori, E. Ohmichi, S. Ikeda, S. NishiZaki, and S. Nakatsuji, *Phys. Rev. Lett.* **81**, 3765 (1998).

<sup>18</sup>M.G. Hildebrand, M. Reedyk, T. Katsufuji, and Y. Tokura, *Phys. Rev. Lett.* **87**, 227002 (2001).

<sup>19</sup>K. Pucher, A. Loidl, N. Kikugawa, and Y. Maeno, *Acta Phys. Pol. B* **34**, 587 (2003).

<sup>20</sup>M. Minakata and Y. Maeno, *Phys. Rev. B* **63**, 180504 (2001).

<sup>21</sup>K. Pucher, J. Hemberger, F. Mayr, V. Fritsch, A. Loidl, E.W.

- Scheidt, S. Klimm, R. Horny, S. Horn, S.G. Ebbinghaus, A. Reller, and R.J. Cava, *Phys. Rev. B* **65**, 104523 (2002).
- <sup>22</sup>M. Braden, O. Friedt, Y. Sidis, P. Bourges, M. Minakata, and Y. Maeno, *Phys. Rev. Lett.* **88**, 197002 (2002).
- <sup>23</sup>Z. Mao, Y. Maeno, and H. Fukazawa, *Mater. Res. Bull.* **35**, 1813 (2000).
- <sup>24</sup>N. Kikugawa and Y. Maeno, *Phys. Rev. Lett.* **89**, 117001 (2002).
- <sup>25</sup>M. Braden (unpublished).
- <sup>26</sup>T. Timusk, S.L. Herr, K. Kamaras, C.D. Porter, D.B. Tanner, D.A. Bonn, J.D. Garrett, C.V. Stager, J.E. Greedan, and M. Reedyk, *Phys. Rev. B* **38**, 6683 (1988).
- <sup>27</sup>D.J. Singh, *Phys. Rev. B* **52**, 1358 (1995).
- <sup>28</sup>A.P. Mackenzie, S.R. Julian, A.J. Diver, G.J. McMullan, M.P. Ray, G.G. Lonzarich, Y. Maeno, S. NishiZaki, and T. Fujita, *Phys. Rev. Lett.* **76**, 3786 (1996).
- <sup>29</sup>B.I. Barker, S.K. Dutta, C. Lupien, P.L. McEuen, N. Kikugawa, Y. Maeno, and J.C. Davis, *Physica B* **329-333**, 1334 (2003).
- <sup>30</sup>T. Valla, P.D. Johnson, Z. Yusof, B. Wells, Q. Li, S.M. Loureiro, R.J. Cava, M. Mikami, Y. Mori, M. Yoshimura, and T. Sasaki, *Nature (London)* **417**, 627 (2002).